

Article

Fluorine-Free Plasma Polymers to Obtain Water-Repellent Cotton Fabrics: How to Control Their Durability?

Syrine Jebali ^{1,2}, Jamerson Carneiro de Oliveira ¹, Aissam Airoudj ¹, Asma Riahi ¹, Philippe Fioux ¹, Fabrice Morlet-Savary ¹, Ludovic Josien ¹, Isabelle Ferreira ², Vincent Roucoules ¹ and Florence Bally-Le Gall ^{1,*}

¹ Université de Haute-Alsace, Université de Strasbourg, CNRS, IS2M UMR 7361, 15 rue Jean Starcky, F-68100 Mulhouse, France; syrinejebali93@gmail.com (S.J.); jamerson.carneiro-de-oliveira@uha.fr (J.C.d.O.); aissam.airoudj@uha.fr (A.A.); asma.riahi@uha.fr (A.R.); philippe.fioux@uha.fr (P.F.); fabrice.morlet-savary@uha.fr (F.M.-S.); ludovic.josien@uha.fr (L.J.); vincent.roucoules@uha.fr (V.R.)

² Institut Français du Textile et de l'Habillement (IFTH), 185 rue de l'Illberg, F-68200 Mulhouse, France; iferreira@ifth.org

* Correspondence: florence.bally-le-gall@uha.fr

Abstract: The plasma polymerization of hexamethyldisiloxane (HMDSO) leads to the environmentally friendly fabrication of water-repellent coatings through a vapor-phase surface functionalization process using alternatives to the controversial perfluoroacrylate precursors. However, the durability of these coatings is their Achilles' heel, which requires an in-depth study of the relationship between the structure and properties of these thin films in order to propose concrete solutions for the fabrication of fluorine-free water-repellent textiles. In this context, HMDSO plasma polymers have been deposited on cotton fabrics in an original reactor that allows easy tuning of temporal and spatial parameters of the glow discharge. The functionalized fabrics were characterized to gain insights into the chemical composition of the coatings, their morphology and, above all, their adhesion properties. Interestingly, the results after washing tests revealed a significant dependence of the durability of the superhydrophobic property on the elastic modulus of the deposited polymer. The formation of some radicals at the substrate–thin film interface in the early stages of deposition also correlates with some results. These relationships between the operating conditions of the plasma polymerization, the interfacial properties and the performances of the functionalized fabrics, but also the characterization methodology developed in this work, can undoubtedly serve the engineering of water-repellent fluorine-free coatings on fabrics with optimal durability.

Keywords: HMDSO; low-pressure plasma polymerization; superhydrophobic coating; cotton fabrics; thin film; durability; washing resistance



Citation: Jebali, S.; Carneiro de Oliveira, J.; Airoudj, A.; Riahi, A.; Fioux, P.; Morlet-Savary, F.; Josien, L.; Ferreira, I.; Roucoules, V.; Bally-Le Gall, F. Fluorine-Free Plasma Polymers to Obtain Water-Repellent Cotton Fabrics: How to Control Their Durability?. *Coatings* **2023**, *13*, 1827. <https://doi.org/10.3390/coatings13111827>

Academic Editor: Alexandra Muñoz-Bonilla

Received: 24 September 2023

Revised: 20 October 2023

Accepted: 23 October 2023

Published: 25 October 2023



Copyright: © 2023 by the authors. Licensee MDPI, Basel, Switzerland. This article is an open access article distributed under the terms and conditions of the Creative Commons Attribution (CC BY) license (<https://creativecommons.org/licenses/by/4.0/>).

1. Introduction

Inspired by nature [1–3], the development of synthetic superhydrophobic surfaces is of major concern for the textile industry to achieve water-repellent and self-cleaning properties of its products [4]. Basically, such superhydrophobic surfaces can be obtained by considering two major issues: preparing a dual-scale textured surface and lowering the surface energy via chemical modification. While the inherent structure of the fibers in textile fabrics already contributes to the desired hierarchical structuring of the material, especially in the case of nanostructured fibers [5], their chemical surface modification is a crucial step to achieving superhydrophobic properties. The deposition of a low surface energy coating can be performed, for instance, by using polymer grafting [6–8], sol–gel technique [9,10], dip-coating [11], spray-coating [12,13], chemical vapor deposition [14,15], or plasma treatments [16–19]. Among these techniques, the plasma polymerization process has been identified as a good candidate to engineer such coatings. Indeed, this chemical vapor-phase deposition technique basically leads to the formation of polymer thin films, typically having a thickness of a few nanometers to a few microns, that can be deposited

onto the surface of materials, possibly having relatively complex geometries [20,21]. The use of cold plasma makes possible the treatment of a wide variety of materials, including heat-sensitive materials such as synthetic polymers or cotton, which are widely used in the textile industry [22,23]. Furthermore, this technique is considered to be an environmentally friendly process that does not require the use of solvents. Depending on the choice of organic precursor and the operating conditions used, the nature of the functional groups present in the polymer coating can be tailored to achieve the desired surface chemistry [24]. For example, by modifying the energy supplied to the precursor, different plasma chemistries can be generated, resulting in different chemical compositions and physical properties of the plasma polymer, which ultimately affect the coating performances [25,26]. Pulsed plasma polymerization, consisting of generating pulses of plasma discharge, is commonly used to reduce the total energy supplied to the precursor. In this way, a temporal control of plasma polymerization can be achieved [27,28]. In addition, it is well-described in the literature that the deposition mechanisms of plasma polymers depend on the position of the sample within the reactor. For instance, it is known that performing plasma polymerization in the post-discharge zone (also known as remote plasma deposition) limits the crosslinking of plasma polymers since fewer ions are found far from the glow discharge, thus leading to spatial control of plasma polymerization [29]. Consequently, the composition of the plasma discharge depends on a multitude of parameters, such as the power supplied by the electromagnetic wave generator, the pressure in the reactor, and the temporal and spatial parameters of the discharge [30,31].

Several precursors have been reported to deposit superhydrophobic coatings at low and atmospheric pressure, including hydrocarbons [32,33], fluorinated compounds [16,34,35] and organosilicon compounds [36–38]. Although fluorinated compounds with C8 chemistry (with ≥ 8 fluorinated carbon atoms) are among the most widely used in plasma treatments to produce superhydrophobic textiles, these precursors are banned by European regulations and need to be replaced due to their harmful effects on health and the environment [39]. Silicone chemistry has gained attention to provide alternatives to fluorinated compounds, and hexamethyldisiloxane (HMDSO) is one of the most widely used organosilicon precursors to obtain superhydrophobic coatings because of its suitable vapor pressure, low toxicity, commercial availability, and convenient deposition rate. In addition to water repellency, the durability of this property is a requirement, as textiles are subjected to numerous washing cycles, which cause significant mechanical stress. Although some studies have provided data to address this issue for HMDSO plasma polymers [21,40–42], the factors governing the adhesion and cohesion of the superhydrophobic thin films on textile fabrics remain unclear. This lack of understanding is all the more disturbing given that the durability of HMDSO plasma polymers is often considered to be one of their weak points, particularly when compared with fluorinated coatings.

Therefore, our contribution in this field focuses on the attempt to understand the role of a spatial and temporal parameter of the plasma discharge on the performance and durability of the superhydrophobic coatings synthesized via the plasma polymerization of HMDSO on cotton fabrics. For this purpose, low-pressure (pulsed) plasma polymerization of HMDSO has been performed by placing the textile sample at different positions relative to the plasma discharge and by varying the duty cycle of the generator, thus controlling the plasma pulse time. The properties of the HMDSO plasma polymers were systematically studied using infrared and X-ray photoelectron spectroscopies and water contact angle measurements. The durability of the coatings was then tested by performing standard washing cycles and analyzing the samples after washing. An attempt is made to provide quantitative data on the properties that determine the resistance of the coating, namely its cohesion and adhesion to the cotton fabric. More precisely, the mechanical properties of the HMDSO plasma polymers have been investigated using atomic force microscopy, and electron paramagnetic spectroscopy has been tested to try to detect the formation of radicals on cotton in the early stages of polymerization. All these data help to understand

the main parameters that determine the resistance of the coating to washing and, thus, the durability of the water repellency.

2. Materials and Methods

2.1. Deposition of HMDSO Plasma Polymer by Plasma Polymerization

Hexamethyldisiloxane (HMDSO), $C_6H_{18}OSi_2$, ($\geq 98.5\%$, Sigma Aldrich, Darmstadt, Germany), was used as the monomer for surface modification via plasma polymerization. Plasma polymerization experiments were carried out in a unique, home-built RF plasma reactor operating at low pressure. HMDSO plasma polymers were deposited on $1 \times 1 \text{ cm}^2$ single side-polished silicon wafers (100, Si-Mat, Kaufering, Germany) as model substrates for some characterization techniques. They were washed with ethanol and acetone before use. HMDSO plasma polymers were also deposited on $2 \times 2 \text{ cm}^2$ cotton fabrics for water-repellency and durability tests. The chamber consists of a quartz tube (100 cm long and 6 cm diameter) coupled with an externally wound copper coil. A Pirani pressure gauge in series with a two-stage rotary pump (E2M 18, Edwards, Lutín, Czech Republic) connected to a liquid nitrogen cold trap completes the reactor. All components are assembled with grease-free Cajon fittings. An L-C matching network (VM 1500W-ICP, Dressler, Shenzhen, China) is used to match the impedances of the generator (Cesar 133, 13.56 MHz, Dressler, Shenzhen, China) and the reactor by minimizing the standing wave ratio of the transmitted power. Using an oscilloscope, the shape of the pulses during deposition was controlled, and the average power W delivered to the system was calculated according to Equation (1), where P_g is the continuous wave power input indicated by the generator, DC is the duty cycle, t_{on} is the plasma pulse-on time, and t_{off} is the plasma pulse-off time:

$$W = P_g \times DC = P_g \times \left[t_{on} / (t_{on} + t_{off}) \right] \quad (1)$$

Prior to each plasma deposition, the reactor was cleaned for at least 30 min using a high-power air plasma treatment ($P_g = 65 \text{ W}$) to ensure the elimination of residues in the reactor. The substrates were then introduced into the chamber by placing them on a glass support in the desired zone of the reactor. Three preferential positions were chosen for this study (Figure 1): P1 in the pre-discharge zone, P3 in the discharge zone located in the middle of the copper coil, and P5 in the post-discharge zone.

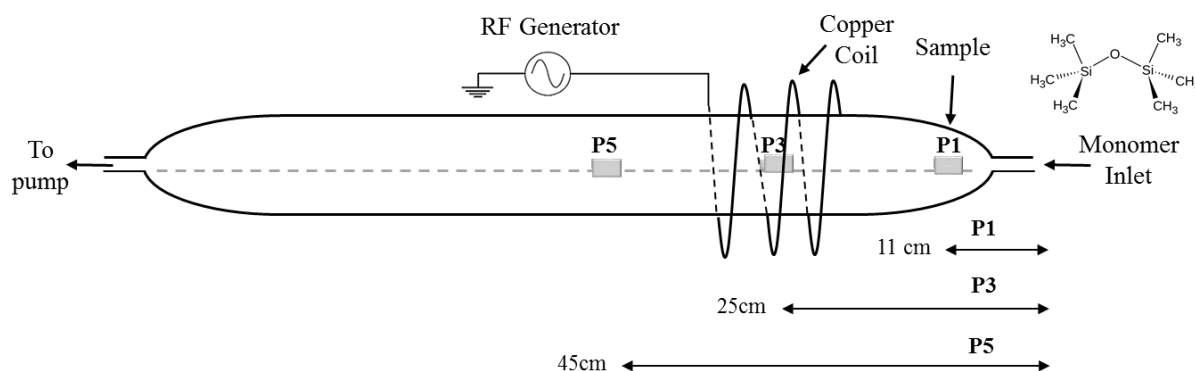


Figure 1. Schematic of the low-pressure plasma reactor used in this work. The different studied positions of the samples are indicated (P1 to P5).

Once a base pressure of about 4×10^{-4} mbar was reached, the introduction of this precursor into the chamber was ensured with a flow controller (Omicron, Eybens, France) at a constant pressure of 0.1 mbar (corresponding to a flow rate of about $42 \mu\text{g}\cdot\text{s}^{-1}$, corresponding to 0.38 sccm). The plasma polymerization was carried out under different conditions of duty cycle $DC = [10\%–100\%]$. The power delivered by the generator and the frequency of the plasma pulses were kept constant at 30 W and 816 Hz, respectively.

2.2. Washing of Cotton Fabrics

The resistance of (plasma-treated) cotton fabrics to washing was investigated by subjecting the samples to successive washing cycles using a standard laundering machine (Electrolux Wascator, Ljungby, Sweden). The small cotton pieces were enclosed in separate small laundry bags, which were carefully sewn onto a raw textile support. The whole support containing the samples was then weighed before dummy wash loads were added to achieve the total two kg required for the laundering test. During one laundering cycle, the samples were first washed using 20 g of IEC A detergent base powder mixed with 5 g of sodium perborate tetrahydrate at 30 °C for 30 min, as described in the NF EN ISO 6330 standard, commonly used in the textile industry. After washing, the samples were allowed to air dry completely before analysis.

2.3. Characterization of HMDSO Plasma Polymer Thin Films

2.3.1. Atomic Force Microscopy (AFM)

AFM was used to determine the elastic moduli of the coatings deposited on silicon wafers and of the cotton fiber using a Bruker Multimode IV with a Nanoscope V controller and an E “vertical” scanner (Bruker, Santa Barbara, CA, USA) via the Peak Force Quantitative Nanomechanical Mapping (PF-QNM, Bruker, Santa Barbara, CA, USA) method. A calibration procedure consisting of precise measurements of tip radius, spring constant and resonance frequency was first performed. All quantitative measurements were carried out with an RTESPA cantilever (Bruker) with a spring constant of 40 N m⁻¹ and a resonance frequency of 300 kHz, a width of 40 μm and a length of 125 μm. Using the Sader method, the actual spring constant was determined and found to be approximately 19 N m⁻¹. The deflection sensitivity (approximately 28 nm V⁻¹) was measured on a silicon surface. The tip radius was calibrated against a polystyrene standard provided by Bruker. The measured tip radius was 70 nm. The Poisson’s ratio was assumed to be 0.3. To obtain relevant results, the cantilever and tip geometry are taken into account in the PF-QNM measurements. Data processing and analysis were performed using Gwyddion software (version 2.62). In particular, the average Young’s modulus, measured at each point of a 5 × 5 μm² area, was calculated for at least three different sample positions.

2.3.2. Scanning Electron Microscopy (SEM), Possibly Coupled with Energy Dispersive X-ray (EDX) Spectroscopy

Plasma polymer coatings deposited on cotton fabrics were observed using a JEOL JSM-7900F (Tokyo, Japan) scanning electron microscope. In addition, elemental mapping was performed using a Quantax (Bruker NanoAnalytics, Berlin, Germany) Energy-Dispersive X-ray (EDX) spectrometer to obtain additional information about the deposited coatings, and in particular, the uniformity of the coatings (conformal coverage of the textile fabrics or presence of delamination areas) before and after washing tests.

2.3.3. Water Static Contact Angle Measurements

Static contact angles with deionized water were measured at room temperature (20 °C) using a Drop Shape Analyzer (DSA100, Krüss, Hamburg, Germany) equipped with a CCD video camera. For model substrates, a 2 μL water droplet was deposited on the surface of the coating. For textiles, the droplet volume was increased to 5 μL. The calculated contact angles were the average of the angles measured on both sides of at least seven droplets deposited at different locations on the sample. The ellipse tangent⁻¹ method was used to determine all angles.

2.3.4. Electron Paramagnetic Resonance (EPR) Spectroscopy

EPR spectroscopy was carried out using an X-Band EMX-plus spectrometer (Bruker Biospin, Wissembourg, France). The (treated) cotton samples were removed from the plasma reactor and immediately immersed in liquid nitrogen to minimize the reaction of radicals present on the surface of the sample with air (contact time with air less than

15 s). The sample was stored in liquid nitrogen until the start of the measurement (except for one sample, presented in Supporting Information, to verify the influence of the delay time between the removal of the sample from liquid nitrogen and the start of the spectrum acquisition on the shape of the EPR spectrum).

3. Results and Discussion

3.1. Evaluation of the Durability of HMDSO Plasma Polymers Deposited on Cotton Fabrics

3.1.1. Development of Water-Repellent Plasma Polymer Coatings on Cotton Fabrics

The plasma polymerization of HMDSO has been performed on cotton fabrics in an original plasma reactor, which provides the possibility of investigating the temporal and spatial dependence of the plasma discharge on the thin film properties [30,31]. The temporal control of the (pulsed) plasma polymerization was ensured by changing the duty cycle (DC) of the generator (DC = 10%, 50% and 100%). The positioning of the samples in the different zones of the reactor (in the pre-discharge zone P1, the discharge zone P3 and the post-discharge zone P5) offers the possibility to study the spatial dependence of the plasma polymerization simultaneously to the temporal dependence. To verify the presence of HMDSO plasma polymers (with comparable thicknesses close to 170 nm) on the fabrics, ATR-FTIR analyses were performed on all samples and the characteristic vibrational bands of the HMDSO plasma polymer were detected in addition to the spectrum of the pristine cotton (see Figure S1 in Supporting Information). SEM images taken at several magnifications also confirm the presence of a coating on the cotton fabrics after plasma polymerization of HMDSO (see Figure S2 in Supporting Information). Interestingly, they also enabled us to visualize that the dual-scale structuring of the textile fabrics at the microscale, but also at the nanoscale, coming from the microfibril bundles of the cellulose fibers [5], seems to be preserved after the deposition of the plasma thin film. This morphology is of particular interest for the targeted application of these plasma polymers as water-repellent coatings. This latter property was evaluated by measuring the water static contact angles on the different coated cotton fabrics, presented in Figure 2. All water contact angles measured on the treated cotton fabrics are higher than 150°, and all water shedding angles [43] were close to 10°, sometimes even lower than 10° (see Figure S3 in Supporting Information). Despite a slight temporal dependence of the chemical composition of the coatings (regarding the XPS and ATR-FTIR analyses given in Tables S1 and S2 and Figures S4–S8 in Supporting Information), these results confirm that an appropriate surface structuring, inherent to the textile fabrics, in combination with the hydrophobicity of HMDSO plasma polymers, synthesized in a specific range of operating conditions, provides the expected water-repellent property to hydrophilic cotton fabrics [21,41]. However, an essential criterion for industrial applications of such coatings for the textile industry is the durability of these wetting properties, especially after washing. This leads to the questions of how HMDSO plasma polymers deposited on cotton fabrics withstand laundering tests and what are the critical parameters influencing their durability. These will be evaluated in the following subsections.

3.1.2. Resistance to Washing Cycles to Evaluate the Durability of Coated Cotton Fabrics

The resistance to washing of HMDSO plasma polymers deposited on cotton fabrics under different operating conditions was studied by subjecting the samples to repeated laundering cycles, also commonly named washing cycles, according to standard procedures used in the textile industry. The measurement of the static contact angle with water was chosen to evaluate the durability of the superhydrophobic properties of the coatings and was therefore performed on each sample after each washing cycle. Figure 2 summarizes the water contact angle values measured on HMDSO plasma polymers synthesized under different conditions (DC = 10%, 50% and 100%, positions: P1, P3 and P5) after different numbers of washing cycles (0, 1, 3, 5, 7 and 10 cycles). First, it should be noted that all coatings at least partially survived one washing cycle since water contact angles higher than 140° were measured on all samples after this first washing cycle. However, it should

be noted that all samples have been slightly affected by this durability test since all water contact angles decrease from at least 10° . More significant differences in the wetting behavior of the HMDSO plasma polymers can be observed by increasing the number of washing cycles.

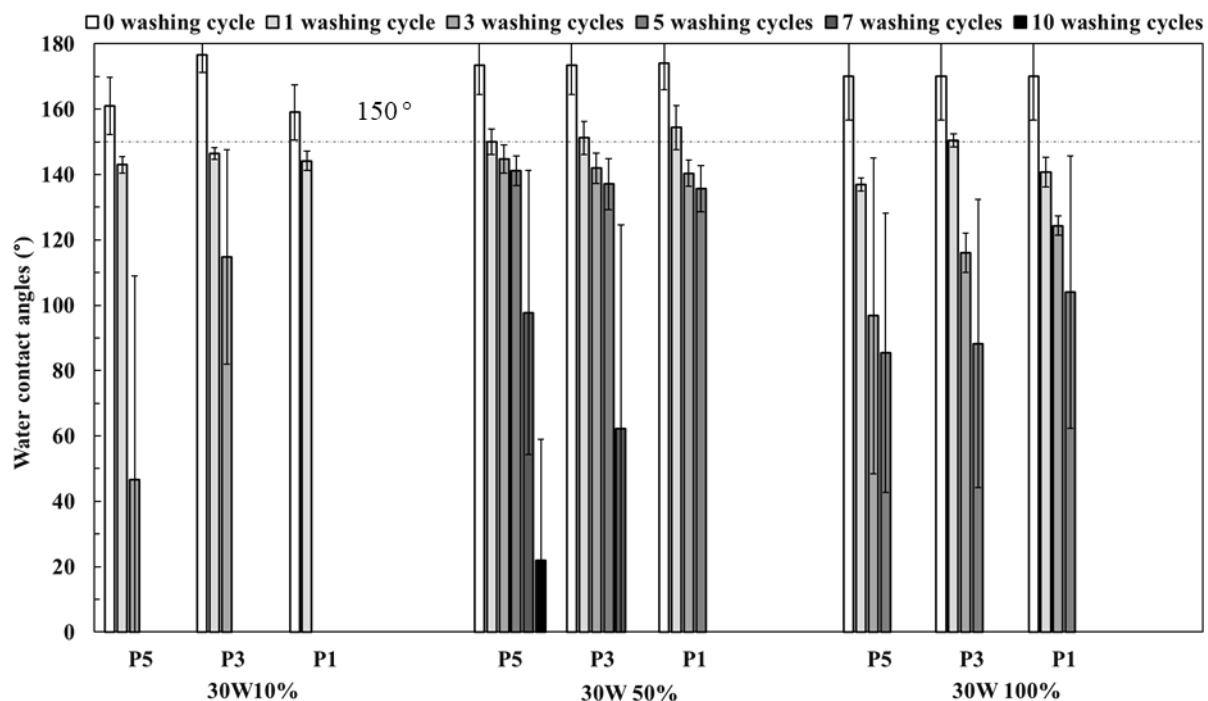


Figure 2. Evolution of water contact angles before and after successive washing cycles performed on cotton fabrics coated with HMDSO plasma polymers deposited at different reactor positions (P1, P3, P5) and different duty cycles (DC = 10, 50 and 100%).

Regardless of the position of the fabrics in the reactor, plasma polymers synthesized at the lowest duty cycle (DC = 10%) have a very low resistance to washing. Indeed, the surface becomes fully hydrophilic after a maximum of three washing cycles. In these cases, water droplets were immediately absorbed into the textile fabrics (no water contact angle value could then be reported in Figure 2), just like the untreated reference. Increasing the duty cycle to 50% leads to a significant increase in the resistance of the coatings to washing since a water contact angle higher than 130° could be measured on the surface of the samples prepared at the different positions in the reactor even after five washing cycles. A further increase in the duty cycle to 100% (corresponding to a continuous deposition mode) did not result in an increase in the water contact angle values measured after washing. Indeed, the water contact angles decreased below 120° after three washing cycles for the samples prepared in all positions in the reactor, and the water contact angle could not be measured after 10 washing cycles. It should be noted that the water shedding angles were also measured on the coated textile fabrics after the washing tests. Only after one washing cycle could a shedding angle of $18 \pm 3^\circ$ be measured for the samples prepared with a 50% duty cycle. For all other samples, the droplets adhered more to the surface, and the water shedding angle exceeded 30° after washing. These results show that a certain heterogeneity appears on the coating as soon as it is subjected to the first washing cycles. At this stage, several questions arise about the origin(s) of the loss of superhydrophobic behavior after washing. Does it come from changes in the chemical composition of the plasma polymer during washing? Are there changes in the structure of the textile fabrics itself due to washing, and/or is it related to a degradation of the fiber/coating interface?

3.2. Understanding the Washing Resistance of HMDSO Plasma Polymers on Cotton Fabrics

3.2.1. Investigation of Possible Chemical and Morphological Changes during Washing

First, the hypothesis of chemical degradation of HMDSO plasma polymer coatings during washing was investigated using ATR-FTIR spectroscopy. The comparison of ATR-FTIR spectra before and after ten laundering cycles did not reveal any drastic changes in the chemical composition of the polymer (see Figure S9 in Supporting Information). However, there is a decrease in the intensity of the signal from the polymer coating compared to the signal from the cotton substrate, likely due to partial removal of the plasma polymer coating from the fabrics during washing. This result is consistent with the loss of water repellency of some samples after several washing cycles.

The morphology of the coated cotton fabrics before and after washing was then characterized by SEM and EDX spectroscopy. Figure 3 presents SEM images and corresponding EDX mappings of the untreated cotton fabric and cotton fabrics treated at two different plasma polymerization conditions, namely DC = 10% and DC = 50% (at position P5). Although a polymer coating is undoubtedly present on the treated cotton fabrics before washing (Figure 3(2.a,3.a)), the morphology of the surface is different after the ten washing cycles (Figure 3(2.b,3.b)). For the lowest duty cycle, the morphology of the fiber after washing is very close to that of the washed untreated cotton fiber, and the EDX mapping shows a surface rich in carbon (red) with a very low content of silicon (blue). This means that the plasma polymer coating has been almost completely removed from the fiber surface after washing.

On the contrary, the morphology of the fabric treated at a 50% duty cycle does not change much after washing, and the EDX mapping still shows the presence of a significant amount of silicon, consistent with the presence of the HMDSO plasma polymer at the fiber surface. These SEM observations and EDX mappings are in agreement with the trends observed through water contact angle measurements and ATR-FTIR spectroscopy. They suggest that the loss of water repellency after several washing cycles is due to the mechanical removal of the plasma polymer coating from the fiber surface due to the aggressive handling conditions of these textile fabrics generated during laundering [44]. In addition, it should be reminded that the macroscopic structure of cotton fabrics is also damaged during laundering (fibers stuck out from the yarn as shown in Figure S10 in Supporting Information), which may also contribute to the drastic loss of superhydrophobicity observed in some coated fabrics after washing.

Thus, the previous characterizations have shown that (i) the loss of superhydrophobic behavior of coated cotton fabrics after washing does not appear to be due to a drastic change in the chemical composition of the plasma polymer coating, and (ii) it may be partially due to the degradation of the microstructure of the textile fabrics, but (iii) the fiber/polymer interface may also be altered after washing. To improve our understanding of the degradation mechanisms occurring during washing, thorough characterizations were attempted to provide additional data on the behavior of the interface.

3.2.2. Determination of Mechanical Properties of HMDSO Plasma Polymers

The rate of polymer crosslinking can greatly affect the cohesion properties of polymer coatings. In addition, the elastic modulus is related to the polymer crosslinking rate. Therefore, quantifying the mechanical elastic properties of plasma polymers can be very useful to indirectly evaluate the cohesion properties of plasma coatings [45]. Consequently, the determination of the elastic modulus of the different plasma polymers was performed using AFM in Peak Force QNM mode, as shown in Table 1. To obtain valuable and reproducible data, these measurements were performed on plasma polymers with a thickness of at least 250 nm on silicon wafers. The results clearly show a significant increase in Young's modulus from about 100 MPa for samples prepared at DC = 10% to about 1350 MPa for samples prepared at DC = 100%. However, it should be noted that the Young's modulus values are rather similar regardless of the position of the sample in the reactor. With a stiffness variation of more than a decade between plasma polymers synthesized at different

duty cycles, it is reasonable to consider this temporal parameter of the plasma discharge as a key element in controlling the final superhydrophobic properties of HMDSO-based coatings. With this chemical composition of the polymer thin film, an intermediate value of Young's modulus, close to 500 Mpa, seems to be ideal to give the coating sufficient cohesion without making it brittle. In other words, if the duty cycle is too low, a weaker crosslinked plasma polymer will be synthesized, resulting in faster removal of the plasma polymer from the cotton fabrics during the washing tests. Conversely, if the duty cycle is too high, the plasma polymer will be over-crosslinked and, therefore, more fragile, which also has a negative effect on the washing resistance of the coating on cotton fabrics.

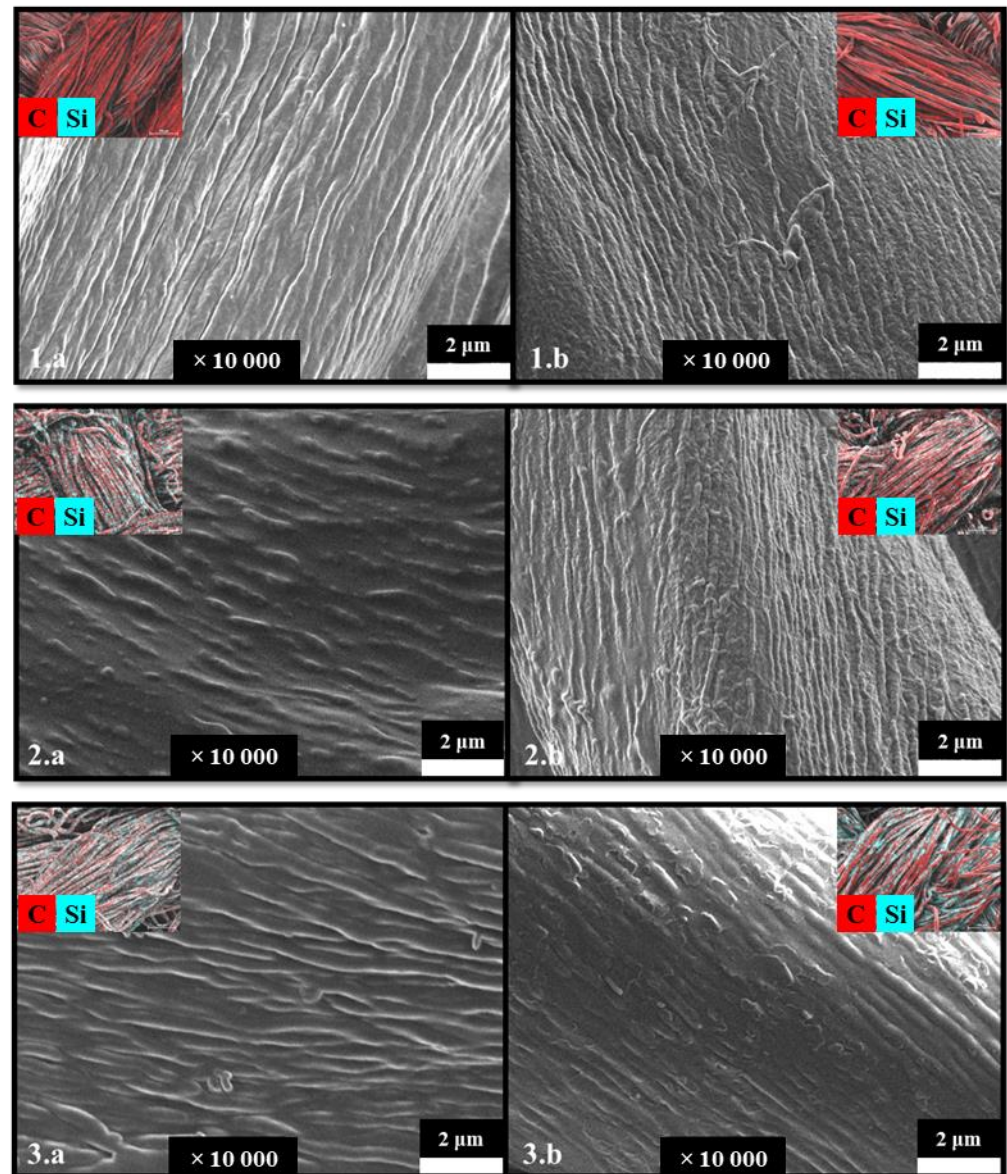


Figure 3. SEM images and corresponding EDX mappings (given as insets; the red color represents carbon, and the blue color represents silicon) of the pristine cotton fabric (1) and HMDSO plasma polymer deposited on cotton fabrics at DC = 10% at position P5 (2) and at DC = 50% at position P5 (3) before washing (a) and after 10 washing cycles (b).

Table 1. AFM (Peak Force QNM) estimation of Young's modulus of HMDSO plasma polymers synthesized under different operating conditions.

Young's Modulus (MPa)	P1	P3	P5
30 W 10%	67 ± 5	125 ± 10	96 ± 13
30 W 50%	666 ± 65	347 ± 33	440 ± 38
30 W 100%	1303 ± 82	1355 ± 103	1402 ± 119

In addition, the interfacial adhesion between a coating and its substrate can also be influenced by their respective mechanical properties. More precisely, it has been demonstrated that the difference in stiffness or elastic modulus between a coating and its substrate is a key parameter when studying friction and wear properties. A large elastic modulus mismatch between the coating and the substrate likely induces interface damage when an external force is applied [46]. To this end, an attempt was made to estimate the Young's modulus of the cotton fiber by AFM and its value was found to be 450 ± 150 MPa (see Figure S11 in Supporting Information). It can be seen that the Young's moduli of the different plasma polymer coatings are very similar to that of the cotton fiber. This result should provide a reasonable continuity in the elastic properties of the polymer coatings and their substrate. It was observed that the HMDSO plasma polymer synthesized at a duty cycle of 50%, which had the better washing resistance, has a Young's modulus value that best matched that of the cotton fiber. Thus, minimal stress at the coating–fiber interface during washing is expected for the HMDSO plasma polymer synthesized at DC = 50%.

At this point, we have shown that the mechanical properties of the different HMDSO plasma polymers differ as a function of the duty cycle, which is likely to affect both the cohesion and adhesion properties of the coatings on cotton fibers. However, the study of the interfacial adhesion of polymeric coatings with a thickness of about 200 nm with a polymeric substrate, namely cotton fiber, remains very challenging.

3.2.3. Indirect Evaluation of the Interface Quality of HMDSO Plasma Polymers—Cotton Fibers by EPR Spectroscopy

Although a direct evaluation of the interfacial adhesion could not be achieved, an indirect characterization of the quality of this interface is proposed. Plasma polymers usually adhere to their substrate due to the formation of radicals on the surface of the substrate from the early stages of plasma polymerization [47], thus creating chemical anchoring points of the coating on the substrate. Therefore, we attempted to characterize the first radicals formed on the surface of the cotton fibers using Electron Paramagnetic Resonance (EPR) spectroscopy. For this purpose, EPR spectra were recorded on cotton fabric samples placed at different positions in the reactor and exposed for 30 s to an HMDSO plasma generated at DC = 50%. These initial radicals generated on the surface of the cotton fabrics were thought to play a crucial role in the adhesion phenomena between the polymer coating and the fiber. Identifying the chemical nature of these reactive species can shed light on the adhesion mechanisms and also help to interpret the results obtained during washing tests. It was particularly interesting to focus this study on samples prepared at a similar specific energy (or duty cycle) provided by the generator but located in different reactor zones. Indeed, for a given specific energy, some differences were observed in terms of resistance to washing, in particular for the most interesting operating condition, namely DC = 50%. Since the values of the Young's moduli were very similar, whatever the position, it is relevant to try to discriminate these samples by using another property to correlate the durability results (resistance to washing).

First, it can be noted that the EPR spectrum of the untreated cotton fabrics showed no signal, indicating the absence of free radicals prior to plasma treatment. Considering the risk of radical recombination upon exposure to air, the samples were frozen and stored in liquid nitrogen immediately after plasma treatment. Figure 4 shows the EPR spectra of cotton fabrics after 30 s of HMDSO plasma exposure at DC = 50% for the three reactor

zones (P1, P3 and P5). The spectra show distinct peaks indicating the presence of different types of radicals on the cotton fabrics. Three lines, labeled I, II and III, can be distinguished. Table 2 summarizes the g-factors, also named Landé factors, calculated for each peak in the EPR spectra of the different samples. This g-factor is calculated with the value of the associated magnetic field and is characteristic of a given radical.

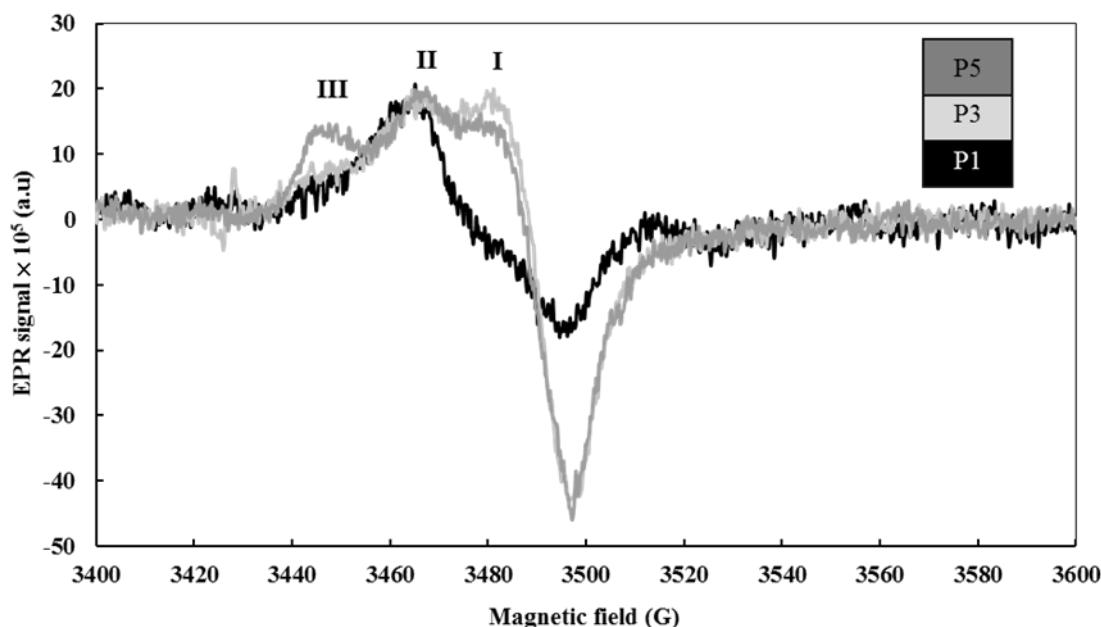


Figure 4. EPR spectra of cotton fabrics treated for 30 s with HMDSO plasma DC = 50% at different positions in the reactor.

Table 2. g-factor values of the different radical species calculated from EPR spectra of cotton fabrics treated at different positions in the reactor (DC = 50%).

Detected Species	Magnetic Field (G)	g-Factor
I	3490	2.006
II	3480	2.014
III	3450	2.030

The g-factor of the first species (I), about 2.006, can be assigned to silyl radicals $R_3Si\bullet$. The presence of this type of radicals in HMDSO plasmas is well described due to the fragmentation of the HMDSO molecule. Many studies have suggested that $\bullet(CH_3)_2SiO\bullet$ biradicals are the predominant species controlling film formation. Thus, the presence of silicon-centered radicals on the fiber surface was expected and is clearly visible, at least in samples prepared in the discharge and post-discharge zones. Moreover, previous EPR studies reporting on cotton irradiation attributed the signal at $g = 2.006$ to the presence of carbon-centered radicals produced in the cotton cellulose [48]. Such radicals are likely to be present on the fiber surface after exposure to HMDSO plasmas. In general, a g-factor of 2.01 could be assigned to $RO\bullet$ or $ROO\bullet$ [49]. Peroxy radicals ($ROO\bullet$) are easily formed by the extremely rapid coupling of C-centered radicals with dioxygen, which can occur during the brief contact with air (for sample retrieval) or, in our case, during plasma exposure, as a small amount of dioxygen may be present in the reactor. Furthermore, alkoxy radicals can be formed during plasma exposure and can be stabilized and thus detected using EPR spectroscopy thanks to the semi-crystalline structure of cellulose [50]. Moreover, it has been reported that two different g-factors can be attributed to peroxy radicals present in cellulose: $g_{//} (=2.01)$ and $g_{\perp} (=2.03)$ [51,52]. Therefore, both species II and III can correspond to peroxy radicals (see also Figure S12 in Supporting Information). It is noteworthy that

the EPR absorption peak at the position of g_{\perp} , corresponding to peroxy radicals, was mainly observed in the sample prepared at P5. As a reminder, the results of resistance to washing showed the best durability of water repellency for the sample prepared in the post-discharge zone. The presence of these radicals, especially in the sample prepared at P5, may explain the good resistance to washing of this specific sample.

In summary, even if EPR spectroscopy has not been able to precisely quantify the number of radicals present in treated cotton fabrics, it has been able to provide additional information on the presence of some types of radicals on cotton fibers and could help in the interpretation of the durability tests previously presented. More precisely, the more significant presence of the third species (III) seems to correlate with the results of the washing resistance tests.

4. Conclusions

The functionalization of cotton fabrics with HMDSO plasma polymers was studied in an original one-meter-long reactor to produce durable water-repellent textile fabrics. Due to the homogeneous extension of the glow discharge within the reactor chamber, the chemical, physicochemical and physical properties of the coatings were found to be rather independent of the position of the sample in the reactor. On the contrary, some differences were observed between plasma polymers synthesized at different duty cycles. While these differences do not significantly affect the initial wettability properties of the treated cotton fabrics, the temporal dependence of the HMDSO plasma polymerization was clearly demonstrated by investigating the durability of the water repellency of the treated cotton fabrics through successive washing cycles. These results can be correlated to differences in cohesion and, to some extent, interfacial adhesion of the HMDSO plasma polymers. Changing the duty cycle used for plasma polymerization has a strong influence on the washing resistance of the plasma polymer. An intermediate duty cycle of 50% (for an input power of the generator of 30 W) seems to provide an optimal cohesion of the coating, evaluated by Young's modulus (close to 500 MPa in this case) by AFM. Moreover, slight differences in the durability of the water-repellency properties could also originate from the different nature of the radicals, identified via EPR spectroscopy for different positions of the sample in the reactor, which are produced at the surface of the cotton fabrics in the early stages of plasma polymerization. Thanks to this in-depth study of the (pulsed) plasma polymerization of HMDSO performed in a unique reactor; it has been possible to produce water-repellent coatings on cotton fabrics that meet many ecological requirements (green process, non-fluorinated precursor) and achieve interesting durability to washing.

Supplementary Materials: The following supporting information can be downloaded at: <https://www.mdpi.com/article/10.3390/coatings13111827/s1>, Figure S1: ATR-FTIR spectra of untreated cotton fabrics and treated ones with HMDSO plasma polymers deposited at different duty cycles; Figure S2: SEM images at different magnifications of cotton textile fabrics before (a) and after (b) plasma polymerization of HMDSO; Figure S3: Water static contact angles and water shedding angles measured on HMDSO plasma polymers deposited on cotton fabrics in different conditions; Figure S4: Typical ATR-FTIR spectrum of HMDSO (a) and HMDSO plasma polymer (b); Figure S5: Evolution of the $R_{2/3}$ ratio of the intensities of the bands at 800 cm^{-1} and 840 cm^{-1} measured in ATR FTIR spectra of HMDSO plasma polymers synthesized using different duty cycles at the different positions in the reactor; Figure S6: Typical XPS survey wide scan (a) and high-resolution spectra of the C1s (b) and Si2p (c) peaks of an HMDSO plasma polymer; Figure S7: (a) Deconvolution of high-resolution spectra of the Si2p of HMDSO plasma polymer and (b) silicon chemical environments and respective binding energies considered for this deconvolution; Figure S8: Relative areas of different silicon chemical states identified in the high-resolution Si2p peak (measured by XPS) of HMDSO plasma polymers prepared using different duty cycles at different positions in the reactor; Figure S9: ATR-FTIR spectra of untreated cotton fabrics and treated ones with HMDSO plasma polymers deposited at different duty cycles before (a) and after 10 washing cycles (b); Figure S10: SEM images at different magnifications of untreated cotton textile fabrics before (a) and after 10 washing cycles (b); Figure S11: 2D and 3D elastic modulus mapping of a single cotton fiber obtained by AFM in Peak Force QNM

mode; Figure S12: EPR spectra of cotton fabrics treated at DC = 50% and P5 measured directly after sample retrieval from the reactor and 6 minutes after; Table S1: Values of $R_{2/3}$ ratios corresponding to the intensities ratios of the bands at 1260 cm^{-1} and 1040 cm^{-1} measured in ATR FTIR spectra of HMDSO plasma polymers synthesized at different duty cycles and different positions in the reactor; Table S2: Atomic percentages of Si, C, and O based on the survey spectra as well as the calculated C/Si and O/Si ratios of HMDSO plasma polymers deposited in different operating conditions. (References [53–60] are cited in the Supplementary Materials).

Author Contributions: Conceptualization, S.J., J.C.d.O., I.F., V.R. and F.B.-L.G.; methodology, S.J., J.C.d.O., V.R. and F.B.-L.G.; validation, J.C.d.O., I.F., V.R. and F.B.-L.G.; investigation, S.J., A.A., A.R., P.F., L.J. and F.M.-S.; resources, A.A., A.R., P.F., L.J. and F.M.-S.; data curation, S.J. and F.B.-L.G.; writing—original draft preparation, S.J.; writing—review and editing, J.C.d.O., I.F., V.R. and F.B.-L.G.; visualization, S.J., P.F., L.J. and F.M.-S.; supervision, J.C.d.O., I.F., V.R. and F.B.-L.G.; project administration, I.F. and F.B.-L.G.; funding acquisition, I.F., V.R. and F.B.-L.G. All authors have read and agreed to the published version of the manuscript.

Funding: This research was funded by the Institut Carnot MICA, project SUPERTEX, and the ANRT, grant number 2017/0966.

Institutional Review Board Statement: Not applicable.

Informed Consent Statement: Not applicable.

Data Availability Statement: The data that support the findings of this study are available from the corresponding author upon reasonable request.

Acknowledgments: The authors thank Philippe Kunemann, Simon Gree and Dominique Berling for their help with surface characterization and access to the IS2M characterization platforms. They are also grateful to Alice Broeglin for her technical assistance with washing tests at IFTH Mulhouse.

Conflicts of Interest: The authors declare no conflict of interest.

References

1. Wang, S.; Liu, K.; Yao, X.; Jiang, L. Bioinspired Surfaces with Superwettability: New Insight on Theory, Design, and Applications. *Chem. Rev.* **2015**, *115*, 8230–8293. [[CrossRef](#)] [[PubMed](#)]
2. Kota, A.K.; Kwon, G.; Tuteja, A. The design and applications of superomniphobic surfaces. *NPG Asia Mater.* **2014**, *6*, e109. [[CrossRef](#)]
3. Darmanin, T.; Guittard, F. Superhydrophobic and superoleophobic properties in nature. *Mater. Today* **2015**, *18*, 273–285. [[CrossRef](#)]
4. Li, S.; Huang, J.; Chen, Z.; Chen, G.; Lai, Y. A review on special wettability textiles: Theoretical models, fabrication technologies and multifunctional applications. *J. Mater. Chem. A* **2017**, *5*, 31–55. [[CrossRef](#)]
5. Manley, R.S.J. Fine Structure of Native Cellulose Microfibrils. *Nature* **1964**, *204*, 1155–1157. [[CrossRef](#)]
6. Li, S.H.; Huang, J.Y.; Ge, M.Z.; Li, S.W.; Xing, T.L.; Chen, G.Q.; Liu, Y.Q.; Zhang, K.Q.; Al-Deyab, S.S.; Lai, Y.K. Controlled grafting superhydrophobic cellulose surface with environmentally-friendly short fluoroalkyl chains by ATRP. *Mater. Des.* **2015**, *85*, 815–822. [[CrossRef](#)]
7. Li, Y.; Zheng, X.; Zhu, H.; Wu, K.; Lu, M. Synthesis and self-assembly of well-defined binary graft copolymer and its use in superhydrophobic cotton fabrics preparation. *RSC Adv.* **2015**, *5*, 46132–46145. [[CrossRef](#)]
8. Shang, Q.; Hu, L.; Yang, X.; Hu, Y.; Bo, C.; Pan, Z.; Ren, X.; Liu, C.; Zhou, Y. Superhydrophobic cotton fabric coated with tannic acid/polyhedral oligomeric silsesquioxane for highly effective oil/water separation. *Prog. Org. Coat.* **2021**, *154*, 106191. [[CrossRef](#)]
9. Wang, H.; Ding, J.; Xue, Y.; Wang, X.; Lin, T. Superhydrophobic fabrics from hybrid silica sol-gel coatings: Structural effect of precursors on wettability and washing durability. *J. Mater. Res.* **2010**, *25*, 1336–1343. [[CrossRef](#)]
10. Sfameni, S.; Lawnick, T.; Rando, G.; Visco, A.; Textor, T.; Plutino, M.R. Super-Hydrophobicity of Polyester Fabrics Driven by Functional Sustainable Fluorine-Free Silane-Based Coatings. *Gels* **2023**, *9*, 109. [[CrossRef](#)]
11. Hu, H.; Liu, G.; Wang, J. Clear and Durable Epoxy Coatings that Exhibit Dynamic Omniphobicity. *Adv. Mater. Interfaces* **2016**, *3*, 1600001. [[CrossRef](#)]
12. Wu, X.; Wyman, I.; Zhang, G.; Lin, J.; Liu, Z.; Wang, Y.; Hu, H. Preparation of superamphiphobic polymer-based coatings via spray- and dip-coating strategies. *Prog. Org. Coat.* **2016**, *90*, 463–471. [[CrossRef](#)]
13. Guo, Y.; Li, C.; Li, X.; Xu, H.; Chen, W.; Fang, K.; Zhang, L.; Li, R.; Xie, R. Fabrication of superhydrophobic cotton fabric with multiple durability and wearing comfort via an environmentally friendly spraying method. *Ind. Crop. Prod.* **2023**, *194*, 116359. [[CrossRef](#)]
14. Ma, M.; Mao, Y.; Gupta, M.; Gleason, K.K.; Rutledge, G.C. Superhydrophobic Fabrics Produced by Electrospinning and Chemical Vapor Deposition. *Macromolecules* **2005**, *38*, 9742–9748. [[CrossRef](#)]

15. Zheng, Z.; Gu, Z.; Huo, R.; Ye, Y. Superhydrophobicity of polyvinylidene fluoride membrane fabricated by chemical vapor deposition from solution. *Appl. Surf. Sci.* **2009**, *255*, 7263–7267. [[CrossRef](#)]
16. Balu, B.; Breedveld, V.; Hess, D.W. Fabrication of “Roll-off” and “Sticky” Superhydrophobic Cellulose Surfaces via Plasma Processing. *Langmuir* **2008**, *24*, 4785–4790. [[CrossRef](#)]
17. Caschera, D.; Mezzi, A.; Cerri, L.; de Caro, T.; Riccucci, C.; Ingo, G.M.; Padeletti, G.; Biasiucci, M.; Gigli, G.; Cortese, B. Effects of plasma treatments for improving extreme wettability behavior of cotton fabrics. *Cellulose* **2014**, *21*, 741–756. [[CrossRef](#)]
18. Ma, C.; Nikiforov, A.; Hegemann, D.; De Geyter, N.; Morent, R.; Ostrikov, K. (Ken) Ostrikov, Plasma-controlled surface wettability: Recent advances and future applications. *Int. Mater. Rev.* **2023**, *68*, 82–119. [[CrossRef](#)]
19. Fradin, C.; Salapare, H., III; Amigoni, S.; Guittard, F.; Darmanin, T. Resistant amphiphobic textile coating by plasma induced polymerization of a pyrrole derivative grafted to silica nanoparticles and short fluorinated alkyl chains. *Mater. Today Commun.* **2022**, *30*, 103171. [[CrossRef](#)]
20. Kaplan, S. Plasma processes for wide fabric, film and non-wovens. *Surf. Coat. Technol.* **2004**, *186*, 214–217. [[CrossRef](#)]
21. Kale, K.H.; Palaskar, S. Atmospheric pressure plasma polymerization of hexamethyldisiloxane for imparting water repellency to cotton fabric. *Text. Res. J.* **2011**, *81*, 608–620. [[CrossRef](#)]
22. Morent, R.; De Geyter, N.; Verschuren, J.; De Clerck, K.; Kiekens, P.; Leys, C. Non-thermal plasma treatment of textiles. *Surf. Coat. Technol.* **2008**, *202*, 3427–3449. [[CrossRef](#)]
23. Airoudj, A.; Bally-Le Gall, F.; Roucoules, V. Textile with Durable Janus Wetting Properties Produced by Plasma Polymerization. *J. Phys. Chem. C* **2016**, *120*, 29162–29172. [[CrossRef](#)]
24. Mertz, G.; Delmée, M.; Bardon, J.; Martin, A.; Ruch, D.; Fouquet, T.; Garreau, S.; Airoudj, A.; Marguier, A.; Ploux, L.; et al. Atmospheric pressure plasma co-polymerization of two acrylate precursors: Toward the control of wetting properties. *Plasma Process. Polym.* **2018**, *15*, 1800073. [[CrossRef](#)]
25. Wang, Y.; Zhang, J.; Shen, X. Surface structures tailoring of hexamethyldisiloxane films by pulse rf plasma polymerization. *Mater. Chem. Phys.* **2006**, *96*, 498–505. [[CrossRef](#)]
26. Asadollahi, S.; Profili, J.; Farzaneh, M.; Stafford, L. Development of Organosilicon-Based Superhydrophobic Coatings through Atmospheric Pressure Plasma Polymerization of HMDSO in Nitrogen Plasma. *Materials* **2019**, *12*, 219. [[CrossRef](#)] [[PubMed](#)]
27. Muzammil, I.; Li, Y.P.; Li, X.Y.; Lei, M.K. Duty cycle dependent chemical structure and wettability of RF pulsed plasma copolymers of acrylic acid and octafluorocyclobutane. *Appl. Surf. Sci.* **2018**, *436*, 411–418. [[CrossRef](#)]
28. Teare, D.O.H.; Spanos, C.G.; Ridley, P.; Kinmond, E.J.; Roucoules, V.; Badyal, J.P.S.; Brewer, S.A.; Coulson, S.; Willis, C. Pulsed Plasma Deposition of Super-Hydrophobic Nanospheres. *Chem. Mater.* **2002**, *14*, 4566–4571. [[CrossRef](#)]
29. Blanchard, N.E.; Hanselmann, B.; Drosten, J.; Heuberger, M.; Hegemann, D. Densification and Hydration of HMDSO Plasma Polymers: Densification and Hydration of HMDSO Films. *Plasma Process. Polym.* **2014**, *12*, 32–41. [[CrossRef](#)]
30. Jebali, S.; Airoudj, A.; Ferreira, I.; Hegemann, D.; Roucoules, V.; Gall, F.B.-L. Unique combination of spatial and temporal control of maleic anhydride plasma polymerization. *Plasma Process. Polym.* **2021**, *18*, e2000244. [[CrossRef](#)]
31. Jebali, S.; de Oliveira, J.C.; Airoudj, A.; Josien, L.; Fioux, P.; Ferreira, I.; Roucoules, V.; Bally-Le Gall, F. Thin films deposition versus nanoparticles formation: How can the desired polymer coating be obtained? *Plasma Process. Polym.* **2022**, *19*, e2100091. [[CrossRef](#)]
32. Lee, S.H.; Dilworth, Z.R.; Hsiao, E.; Barnette, A.L.; Marino, M.; Kim, J.H.; Kang, J.-G.; Jung, T.-H.; Kim, S.H. One-Step Production of Superhydrophobic Coatings on Flat Substrates via Atmospheric Rf Plasma Process Using Non-Fluorinated Hydrocarbons. *ACS Appl. Mater. Interfaces* **2011**, *3*, 476–481. [[CrossRef](#)] [[PubMed](#)]
33. Kim, J.-H.; Liu, G.; Kim, S.H. Deposition of stable hydrophobic coatings with in-line CH₄ atmospheric rf plasma. *J. Mater. Chem.* **2006**, *16*, 977–981. [[CrossRef](#)]
34. Graham, P.; Stone, M.; Thorpe, A.; Nevell, T.G.; Tsibouklis, J. Fluoropolymers with very low surface energy characteristics. *J. Fluor. Chem.* **2000**, *104*, 29–36. [[CrossRef](#)]
35. D’agostino, R.; Cramarossa, F.; Colaprico, V.; D’ettolo, R. Mechanisms of etching and polymerization in radiofrequency discharges of CF₄-H₂, CF₄-C₂F₄, C₂F₆-H₂, C₃F₈-H₂. *J. Appl. Phys.* **1983**, *54*, 1284–1288. [[CrossRef](#)]
36. Foroughi Mobarakeh, L.; Jafari, R.; Farzaneh, M. Superhydrophobic Surface Elaboration Using Plasma Polymerization of Hexamethyldisiloxane (HMDSO). *Adv. Mater. Res.* **2011**, *409*, 783–787. [[CrossRef](#)]
37. Cho, S.C.; Hong, Y.C.; Ji, Y.Y.; Han, C.S.; Uhm, H.S. Surface modification of polyimide films, filter papers, and cotton clothes by HMDSO/toluene plasma at low pressure and its wettability. *Curr. Appl. Phys.* **2009**, *9*, 1223–1226. [[CrossRef](#)]
38. Marchand, D.J.; Dilworth, Z.R.; Stauffer, R.J.; Hsiao, E.; Kim, J.-H.; Kang, J.-G.; Kim, S.H. Atmospheric rf plasma deposition of superhydrophobic coatings using tetramethylsilane precursor. *Surf. Coat. Technol.* **2013**, *234*, 14–20. [[CrossRef](#)]
39. Zahid, M.; Mazzon, G.; Athanassiou, A.; Bayer, I.S. Environmentally benign non-wettable textile treatments: A review of recent state-of-the-art. *Adv. Colloid Interface Sci.* **2019**, *270*, 216–250. [[CrossRef](#)]
40. Gotoh, K.; Shohbuke, E.; Ryu, G. Application of atmospheric pressure plasma polymerization for soil guard finishing of textiles. *Text. Res. J.* **2018**, *88*, 1278–1289. [[CrossRef](#)]
41. Yang, J.; Pu, Y.; Miao, D.; Ning, X. Fabrication of Durably Superhydrophobic Cotton Fabrics by Atmospheric Pressure Plasma Treatment with a Siloxane Precursor. *Polymers* **2018**, *10*, 460. [[CrossRef](#)]
42. Rani, K.V.; Chandwani, N.; Kikani, P.; Nema, S.K.; Sarma, A.K.; Sarma, B. Hydrophobic surface modification of silk fabric using plasma-polymerized hmdso. *Surf. Rev. Lett.* **2018**, *25*, 1850060. [[CrossRef](#)]

43. Zimmermann, J.; Seeger, S.; Reifler, F.A. Water Shedding Angle: A New Technique to Evaluate the Water-Repellent Properties of Superhydrophobic Surfaces. *Text. Res. J.* **2009**, *79*, 1565–1570. [[CrossRef](#)]
44. Goynes, W.R.; Rollins, M.L. A Scanning Electron-Microscope Study of Washer-Dryer Abrasion in Cotton Fibers. *Text. Res. J.* **1971**, *41*, 226–231. [[CrossRef](#)]
45. Choukourov, A.; Gordeev, I.; Arzhakov, D.; Artemenko, A.; Kousal, J.; Kylián, O.; Slavínská, D.; Biederman, H. Does Cross-Link Density of PEO-Like Plasma Polymers Influence their Resistance to Adsorption of Fibrinogen? *Plasma Process. Polym.* **2012**, *9*, 48–58. [[CrossRef](#)]
46. Huang, X.; Etsion, I.; Shao, T. Effects of elastic modulus mismatch between coating and substrate on the friction and wear properties of TiN and TiAlN coating systems. *Wear* **2015**, *338–339*, 54–61. [[CrossRef](#)]
47. Ershov, S.; Khelifa, F.; Lemaur, V.; Cornil, J.; Cossement, D.; Habibi, Y.; Dubois, P.; Snyders, R. Free Radical Generation and Concentration in a Plasma Polymer: The Effect of Aromaticity. *ACS Appl. Mater. Interfaces* **2014**, *6*, 12395–12405. [[CrossRef](#)]
48. Sudprasert, W.; Insuan, P.; Khamkhongmee, S. EPR study of free radicals in cotton fiber for its potential use as a fortuitous dosimeter in radiological accidents. *J. Phys. Conf. Ser.* **2015**, *611*, 012012. [[CrossRef](#)]
49. Walton, J.C. Analysis of Radicals by EPR. In *Encyclopedia of Radicals in Chemistry, Biology and Materials*; John Wiley & Sons, Ltd.: Hoboken, NJ, USA, 2012. [[CrossRef](#)]
50. Bernhard, W.A.; Close, D.M.; Hüttermann, J.; Zehner, H. The alkoxy radical, RCH₂O•, as a free radical product in x-irradiated single crystals of nucleosides and nucleotides. *J. Chem. Phys.* **1977**, *67*, 1211–1219. [[CrossRef](#)]
51. Hon, D.N.-S. Photooxidative degradation of cellulose: Reactions of the cellulosic free radicals with oxygen. *J. Polym. Sci. Polym. Chem. Ed.* **1979**, *17*, 441–454. [[CrossRef](#)]
52. Hon, D.N.-S. On the reactivity of cellulose free radicals in graft copolymerization reactions. *J. Polym. Sci. Polym. Chem. Ed.* **1980**, *18*, 1857–1869. [[CrossRef](#)]
53. Zimmermann, J.; Reifler, F.A.; Fortunato, G.; Gerhardt, L.; Seeger, S. A Simple, One-Step Approach to Durable and Robust Superhydrophobic Textiles. *Adv. Funct. Mater.* **2008**, *18*, 3662–3669. [[CrossRef](#)]
54. Chung, C.; Lee, M.; Choe, E.K. Characterization of cotton fabric scouring by FT-IR ATR spectroscopy. *Carbohydr. Polym.* **2004**, *58*, 417–420. [[CrossRef](#)]
55. Raynaud, P.; Despax, B.; Segui, Y.; Caquineau, H. FTIR Plasma Phase Analysis of Hexamethyldisiloxane Discharge in Microwave Multipolar Plasma at Different Electrical Powers. *Plasma Process. Polym.* **2004**, *2*, 45–52. [[CrossRef](#)]
56. Siliprandi, R.A.; Zanini, S.; Grimoldi, E.; Fumagalli, F.S.; Barni, R.; Riccardi, C. Atmospheric Pressure Plasma Discharge for Polysiloxane Thin Films Deposition and Comparison with Low Pressure Process. *Plasma Chem. Plasma Process.* **2011**, *31*, 353–372. [[CrossRef](#)]
57. Socrates, G. *Infrared and Raman Characteristic Group Frequencies: Tables and Charts*; John Wiley & Sons: Hoboken, NJ, USA, 2004.
58. Alexander, M.; Short, R.; Jones, F.; Michaeli, W.; Blomfield, C. A study of HMDSO/O₂ plasma deposits using a high-sensitivity and -energy resolution XPS instrument: Curve fitting of the Si 2p core level. *Appl. Surf. Sci.* **1998**, *137*, 179–183. [[CrossRef](#)]
59. Roualdes, S.; Berjoan, R.; Durand, J. ²⁹Si NMR and Si2p XPS correlation in polysiloxane membranes prepared by plasma enhanced chemical vapor deposition. *Sep. Purif. Technol.* **2001**, *25*, 391–397. [[CrossRef](#)]
60. Dakroub, G.; Duguet, T.; Esvan, J.; Lacaze-Dufaure, C.; Roualdes, S.; Rouessac, V. Comparative study of bulk and surface compositions of plasma polymerized organosilicon thin films. *Surfaces Interfaces* **2021**, *25*, 101256. [[CrossRef](#)]

Disclaimer/Publisher's Note: The statements, opinions and data contained in all publications are solely those of the individual author(s) and contributor(s) and not of MDPI and/or the editor(s). MDPI and/or the editor(s) disclaim responsibility for any injury to people or property resulting from any ideas, methods, instructions or products referred to in the content.